ARTICLE

VEGF expands erythropoiesis via hypoxia-independent induction of erythropoietin in noncanonical perivascular stromal cells

Alissa C. Greenwald[1], Tamar Licht[1], Saran Kumar[1], Sunday S. Oladipupo[2], Seema Iyer[2], Myriam Grunewald[1]*, and Eli Keshet[1]*

Insufficient erythropoiesis due to increased demand is usually met by hypoxia-driven up-regulation of erythropoietin (Epo). Here, we uncovered vascular endothelial growth factor (VEGF) as a novel inducer of Epo capable of increasing circulating Epo under normoxic, nonanemic conditions in a previously unrecognized reservoir of Epo-producing cells (EPCs), leading to expansion of the erythroid progenitor pool and robust splenic erythropoiesis. Epo induction by VEGF occurs in kidney, liver, and spleen in a population of Gli1+SMA+PDGFRβ+ cells, a signature shared with vascular smooth muscle cells (VSMCs) derived from mesenchymal stem cell–like progenitors. Surprisingly, inhibition of PDGFRβ signaling, but not VEGF signaling, abrogated VEGF-induced Epo synthesis. We thus introduce VEGF as a new player in Epo induction and perivascular Gli1+SMA+PDGFRβ+ cells as a previously unrecognized EPC reservoir that could be harnessed for augmenting Epo synthesis in circumstances such as chronic kidney disease where production by canonical EPCs is compromised.

Introduction

Erythropoiesis is a carefully orchestrated process culminating in the generation of mature enucleated RBCs from hematopoietic stem cells (HSCs) via a bipotent megakaryocytic–erythroid progenitor and progressively more differentiated erythroid progenitors. Under normal conditions, the bone marrow (BM) is the major site of adult erythropoiesis, but in cases of BM injury or increased demand for RBC production, the spleen may launch compensatory erythropoiesis in a process known as extramedullary erythropoiesis (EME). Increasing overall erythropoietic output in all cases requires increasing erythropoietin (Epo) production.

Epo is a pleiotropic cytokine promoting and sustaining erythropoiesis at multiple levels. It plays pivotal roles in directing hematopoiesis toward the erythroid lineage (Grover et al., 2014), in expanding the erythroblast pool (von Lindern et al., 2004), and in exerting an antiapoptotic effect (Koury and Bondurant, 1990). A major control of Epo synthesis is its hypoxic induction mediated by stabilization and binding of HIF2α (hypoxia-inducible factor 2α) to the Epo promoter (see Koury and Haase, 2015 for a recent review on Epo regulation by hypoxia). Significantly less is known, however, regarding Epo regulation under normoxia.

Renal peritubular interstitial fibroblast-like cells (Koury et al., 1988; Lacombe et al., 1988; Semenza et al., 1991; Maxwell et al., 1993; Paliege et al., 2010) and, to a lesser extent, hepatocytes (Koury et al., 1991) are the major producers of Epo under hypoxia. The size of the Epo-producing cell (EPC) pool correlates with the total level of Epo transcription and, correspondingly, with overall circulating Epo levels (Obara et al., 2008; Koury and Haase, 2015). Lineage tracing demonstrated that all EPCs share a common FoxD1+ stromal cell progenitor and that modulation of the HIF pathway (i.e., HIF2α stabilization via Von Hippel–Lindau protein inactivation) can recruit multiple subpopulations of stromal cells to the EPC pool, such as renin-producing cells and interstitial fibroblasts (Koury and Haase, 2015; Kobayashi et al., 2016). While renal vascular smooth muscle cells (VSMCs) are also derived from a FoxD1+ stromal cell progenitor, they have not been previously implicated in Epo production.

Damage to EPCs due to fibrosis results in inadequate Epo production, leading to insufficient erythropoiesis. A notable example is anemia associated with chronic kidney disease (CKD), which results from damage to EPCs and their conversion to SMA+ myofibroblasts (Asada et al., 2011; Souma et al., 2013). This has prompted attempts to restore functionality to damaged EPCs, such as through manipulations of the HIF pathway intended to mimic a native hypoxic response (Kurt et al., 2015; Chang et al., 2016; Souma et al., 2016). An alternate possibility shown here is to recruit alternative cell types to the canonical EPC pool inde-

pendent from the HIF pathway. Attractive candidate cell types in this regard are renal mesenchymal and stromal cells derived from a progenitor common to that of canonical EPCs but not previously ascribed to Epo production, such as VSMCs.

Gli1 is a zinc finger transcription factor initially characterized in glioblastoma that was recently identified as a marker of PDGFRβ⁺ mesenchymal stem cell (MSC)–like perivascular cells that localize to the pericyte niche and possess trilineage differentiation potential to chondrocytes, osteoblasts, and adipocytes (Zhao et al., 2014; Kramann et al., 2015, 2016). It was shown that upon organ injury and neovascularization across multiple organs including heart and kidney, resident Gli1⁺ cells expand and become myofibroblasts or VSMCs, migrating from the adventitia to the media and neointimal layers of the vasculature (Kramann et al., 2015, 2016).

Here, we found that vascular endothelial growth factor A (VEGF-A) is capable of increasing Epo production independent from hypoxia. VEGF-A is a secreted growth factor mostly known for its angiogenic activity; yet VEGF possesses many additional activities both vis-à-vis the vascular system and outside of it (see Senger, 2010 for a review on multiple VEGF functions). Nonvascular functions of VEGF are typically mediated by VEGF receptors expressed by a host of nonvascular cells, including HSCs and various cells of the myeloid lineage (Hattori et al., 2001; Gerber et al., 2002; Xue et al., 2009; Rehn et al., 2014). This may also explain apparent effects of VEGF on multiple processes in the hematopoietic cascade (Bautz et al., 2000; Cervi et al., 2007; Huang et al., 2007; Drogat et al., 2010). Like Epo, VEGF can be induced by hypoxia via the HIF/VHL axis, where it acts to improve tissue perfusion by promoting neovascularization (Shweiki et al., 1992; Forsythe et al., 1996). Not surprisingly, therefore, VEGF and Epo are often coinduced in tissues experiencing hypoxia, notably in hypoxic tumors. While in some cancers, observed splenomegaly and EME are correlated with elevated levels of both circulating VEGF and Epo (Baccarani et al., 1978; Xue et al., 2009; Pinczewski and Papadimitriou, 2011; Feng et al., 2013), a causal relationship between the two has not been examined.

We provide the first evidence that VEGF is a potent Epo inducer leading to an overall increase in RBC production independent from hypoxia. Furthermore, we show that VEGF-driven Epo production takes place in a previously uncharacterized perivascular EPC population and is mediated by a noncanonical mode of VEGF signal transduction dependent on platelet-derived growth factor receptor β (PDGFRβ).

Results

VEGF is a potent Epo inducer in kidney, liver, and spleen

To determine whether VEGF may increase circulating levels of Epo independent from hypoxia, we used a transgenic system for conditional and reversible induction of VEGF in adult mice. Briefly, VEGF was induced upon withdrawing tetracycline (Tet) from the drinking water of bitransgenic mice in which a hepatocyte-specific, Tet-regulated transactivator protein drives expression of the main secreted VEGF isoform VEGF-A$_{164}$ (see Materials and methods for experimental details). A hepatic source of ectopic VEGF acting under the liver-enriched activator protein (LAP) promoter

was chosen to secure continuously high steady state levels of circulating VEGF (Dor et al., 2002). VEGF was induced at 6 wk of age, and its levels in blood were monitored weekly with a VEGF-specific ELISA. Steady state levels of circulating VEGF were found to vary among mice in the range of 300–1,100 pg/ml, with the majority exhibiting circulating levels in the 600–1,000 pg/ml range. Induced VEGF in this system is accessible to all remote organs and can be withdrawn at will by readdition of Tet to the drinking water.

As shown in Fig. 1 A, VEGF dose-dependently increased plasma levels of Epo. At the higher VEGF ranges, Epo levels in plasma reached >10-fold higher levels compared with noninduced control littermates. Importantly, ongoing VEGF signaling was required to maintain these elevated levels of circulating Epo, evidenced by its decline within 1 to 2 wk following VEGF withdrawal (Fig. 1 B). To determine the relative contribution of different organs to overall circulating VEGF-induced Epo, both Epo mRNA (Fig. 1 C) and Epo protein (Fig. 1 D) were measured in tissue homogenates of organs known as Epo producers—namely, kidney, liver, and spleen. VEGF-induced Epo production in kidney was reflected in a dramatic, almost 20-fold increase in Epo mRNA and, correspondingly, by a similar increase in Epo protein. A more modest, yet substantial, four- to fivefold increase in Epo production was also observed in liver and spleen.

Epo induction by VEGF takes place under normoxic, nonanemic conditions

The conditional system used to induce VEGF is not associated with tissue hypoxia, which is the major known physiological Epo inducer. Nevertheless, to ensure that Epo induction by VEGF takes place under fully normoxic conditions, kidney, liver, and spleen sections were immunostained for pimonidazole (Hypoxyprobe). Results showed no difference in Hypoxyprobe staining relative to tissue-matched controls (Fig. 1 E). Likewise, the mRNA transcripts of the HIF target genes *Ldh-A*, *Pgk*, and *Glut1* were not elevated in the VEGF-induced kidney, the major site of hypoxic Epo production (Fig. 1 F), corroborating that its induction by VEGF takes place under normoxia. Next, we wanted to rule out that VEGF-induced Epo up-regulation might represent a compensatory response secondary to VEGF-inflicted erythropoietic stress and anemia. Robust Epo up-regulation (Fig. 1 A) was not associated with a statistically significant decrease in RBC count, hematocrit, or hemoglobin (Fig. 1 G).

Because low levels of circulating VEGF are normally found in both humans (mean 154 pg/ml in a meta-analysis by Choi et al., 2016) and mice, it was of interest to determine whether VEGF also mediates homeostatic Epo production. To this end, endogenous VEGF was blocked by its sequestration with a conditionally induced soluble VEGFR1 decoy receptor (sFlt1) functioning as a VEGF trap as described in May et al. (2011) (see Materials and methods for experimental details). Endogenous VEGF blockade had no effect on circulating Epo levels or kidney Epo expression (Fig. S1), arguing against a role for VEGF in homeostatic Epo production.

VEGF induces Epo in a novel EPC population of perivascular stromal cells

Having identified kidney, liver, and spleen as the primary sources of VEGF-induced Epo production, we next determined which cells
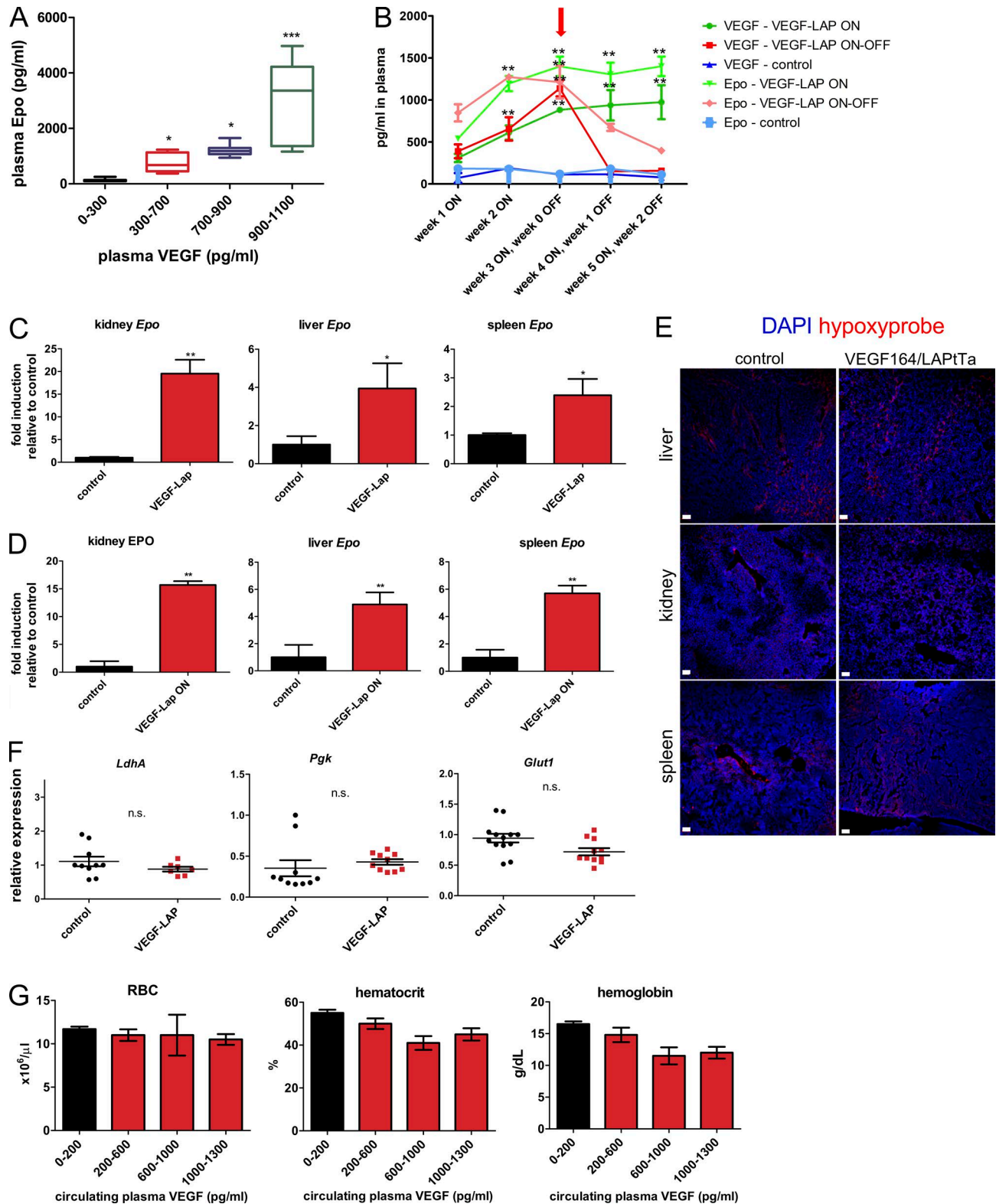
Figure 1. **VEGF induces Epo production by kidney, spleen, and liver under normoxia. (A)** Plasma EPO was determined by ELISA following VEGF induction of TetVEGF164-LAPtTa mice at multiple circulating VEGF levels (n = 10–12 per circulating VEGF concentration group, combining the results of three independent experiments). Statistical analysis was by one-way ANOVA with Tukey post-test. *, P < 0.05; ***, P < 0.001, compared with noninduced control littermates (black); midlines represent median for each group with error bars extending from the first quartile to the minimum and from the third quartile to the maximum. **(B)** Longitudinal weekly measurements of circulating VEGF and Epo levels in noninduced control mice (OFF), VEGF-induced mice (ON), and VEGF-induced mice de-induced 3 wk from induction (arrow; ON–OFF). n = 4–5 mice per group; data are representative of two independent experiments. **, P < 0.01 for comparisons of ON or ON–OFF modes to the corresponding control by unpaired, two-tailed Student's t test; error bars represent SEM. Note rapid decline in circulating Epo upon VEGF de-induction. **(C and D)** Epo mRNA (C) and protein content (D) was measured in kidney, liver, and spleen homogenates derived from control and

Greenwald et al.
VEGF expands erythropoiesis via Epo induction

Journal of Experimental Medicine
https://doi.org/10.1084/jem.20180752

217

in these organs produce Epo under VEGF. Previously, EPCs were identified as intercalated cells of the collecting ducts and proximal and distal tubules under normoxia (Nagai et al., 2014) and as interstitial fibroblast-like cells of the kidney cortex under hypoxia (Lacombe et al., 1988; Pan et al., 2011). Epo immunostaining in kidney sections of VEGF-induced mice revealed multiple EPC populations, including the two mentioned above: CD73+ interstitial fibroblast-like cells (Fig. 2, A, D, E, and G) and DBA+ proximal tubules (Fig. 2 H). Strikingly, an additional previously unrecognized EPC population was discovered—namely, smooth muscle actin+ (SMA+) perivascular stromal cells resembling VSMCs (Fig. 2, A–C, E, and F; and Fig. 3 A). This unique EPC population was also present in VEGF-induced liver and spleen, with EPCs detected in the perivascular niche of nearly all SMA+ vessels but very little to none in littermate controls (Fig. 3, B–D; and Fig. S2).

VEGF recruits alternative EPCs from Gli1+ perivascular MSC-like cells

Recent studies suggested that perivascular Gli1+PDGFRβ+ MSC-like cells may give rise to SMA+ myofibroblasts and to VSMCs (Zhao et al., 2014; Kramann et al., 2015, 2016). We therefore hypothesized that the SMA+ perivascular EPCs described above might also originate from Gli1+ cells. To test this hypothesis, we generated a quadruple transgenic mouse line with the composition Gli1-Cre[ER]::Ai9TdTomato::Tet-VEGF164::LAP-tTA designated for lineage tracing of Gli1+ cells. VEGF was induced by withdrawal of Tet and followed by a tamoxifen pulse to stably label Gli1-expressing cells and their descendants with TdTomato. Triple transgenic mice missing the VEGF responder transgene served as littermate controls (see Fig. 4 A for the experimental scheme). Results showed that VEGF induction led to expansion of the tdTomato-tagged perivascular Gli1+ population at the adventitial and medial layers and was accompanied by acquisition of SMA by these cells (Fig. 4, B and C). Additionally, Gli1+ cells migrated closer to the vasculature, with a more than twofold increase in the percentage of Gli1+ cells that are in direct contact with endothelial cells (Fig. 4, B and D). Remarkably, by 2 wk from the onset of VEGF induction, a significant fraction of the expanded renal Gli1+ population (40%) became Epo positive (Fig. 4, E and F). These results point to perivascular Gli1+ MSC-like cells as a potential source of EPCs that can be recruited by VEGF.

VEGF-induced Epo is not mediated by canonical VEGF receptors but instead by PDGFRβ

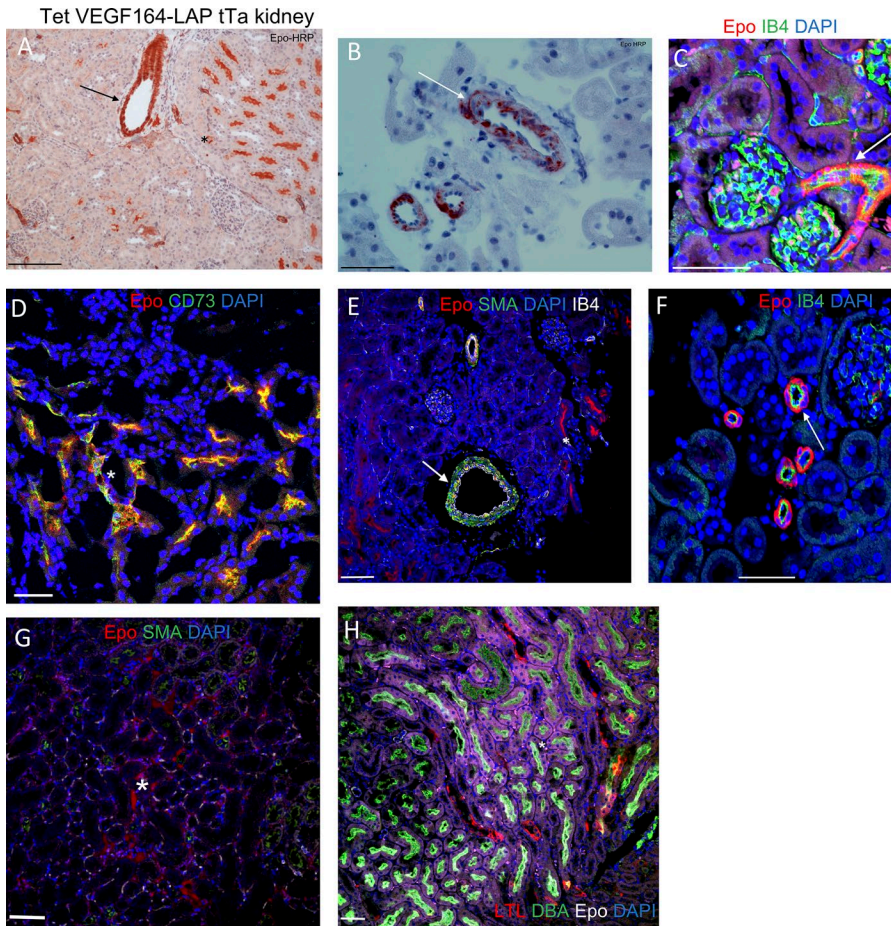We speculated that VEGF signals to Epo-producing SMA+ perivascular stromal cells through its major signaling receptor, Flk1/VEGFR2. However, Flk1/VEGFR2 was undetectable on SMA+ perivascular cells using a Flk1/VEGFR2-GFP knock-in reporter mouse (Fig. 5, A–C). To further examine a mediatory role for canonical VEGF receptors, we measured plasma levels of Epo in VEGF-induced mice treated with the VEGFR1 neutralizing antibody MF1 and the VEGFR2 neutralizing antibody DC101 (Eli Lilly & Co.). Briefly, the respective antibodies were injected i.p. at a dose of 40 mg/kg every 48 h starting 3 wk from VEGF induction, and plasma was drawn for analysis a week later (Fig. 5 D). Up-regulated VEGF-induced Epo was unaffected by VEGFR1 or VEGFR2 neutralization, ruling out their involvement in VEGF signal transduction to SMA+ perivascular cells (Fig. 5, E and F).

Previous studies showed that VEGF can bind and signal directly to PDGFRs in different in vitro contexts including in MSCs (Ball et al., 2007), and can compete with PDGFR-mediated signaling in the vitreous of the eye (Pennock and Kazlauskas, 2012). We therefore examined the possibility that VEGF signals via PDGFRβ to perivascular EPCs in the kidney, liver, and spleen. Indeed, immunostaining demonstrated that VEGF induces PDGFRβ phosphorylation, specifically in SMA+ perivascular cells in all three organs (Fig. 6 A). Notably, this PDGFRβ phosphorylation required continued VEGF signaling and was abolished upon VEGF de-induction (ON–OFF regimen; Fig. S3). To determine whether PDGFRβ is, in fact, required for transducing VEGF signaling to these EPCs, we used an in vivo PDGFRβ neutralization approach. An experimental protocol similar to the one described above for examining a role for VEGF receptors was used except that a PDGFRβ-neutralizing antibody (1B3; Eli Lilly & Co.) replaced VEGF receptor neutralizing antibodies (Fig. 6 B). Results showed that PDGFRβ blockade nullified VEGF-induced Epo mRNA expression in kidney, liver, and spleen (Fig. 6, C–E) and was also reflected in almost no additional increase of circulating VEGF-induced Epo during the 1B3 treatment period (Fig. 6 F). Consistent with our identification of SMA+ perivascular cells as VEGF-recruited EPCs (Figs. 2 and 3), PDGFRβ blockade led to a reduction in the fraction of SMA+ perivascular cells producing Epo, lowering it to the basal noninduced level (Fig. 6, G and H). While our data demonstrate a clear requirement for PDGFRβ in mediating VEGF-induced Epo up-regulation, we cannot distinguish between the possibilities of direct versus indirect signaling.

VEGF-induced Epo acts to boost erythropoiesis in both BM and spleen through expansion of the erythroid progenitor pool

Next, we wanted to determine whether the vast increase in circulating Epo levels induced by VEGF also leads to increased erythropoiesis. Therefore, we examined erythropoiesis in mice exhibiting escalating levels of circulating VEGF compared with

---

VEGF-induced mice. mRNA was quantified by qPCR with GAPDH as a reference, and Epo protein was determined by ELISA. Results are displayed as fold induction relative to the respective level of expression in control littermates ($n = 4$–5 mice for all samples). *, $P < 0.05$; **, $P < 0.01$ by unpaired, two-tailed Student's t test; error bars represent SEM. **(E)** Confocal images of representative kidney, liver, and spleen sections immunostained with Hypoxyprobe (pimonidazole). Data are representative of two independent experiments. Note no significant difference between control and VEGF-induced mice. Bar, 50 µm. **(F)** Normalized relative levels of kidney mRNA of the indicated hypoxia-induced genes measured by qPCR. Each data point corresponds to one animal ($n = 7$–10 mice); data were combined from two independent experiments. n.s., $P > 0.05$ by unpaired, two-tailed Student's t test. n.s., not significant; error bars represent ±SEM. **(G)** RBC, hematocrit, and plasma hemoglobin as a function of circulating VEGF levels, with black representing levels in control mice ($n = 10$ mice per each range of plasma VEGF). Data are representative of two independent experiments. Note no significant difference between each group. $P > 0.05$ by one-way ANOVA with Tukey post-test; error bars represent ±SEM.

Greenwald et al.
VEGF expands erythropoiesis via Epo induction

Journal of Experimental Medicine 218
https://doi.org/10.1084/jem.20180752

Tet VEGF164-LAP tTa kidney

Figure 2. Identification of EPCs in VEGF-induced kidney. VEGF-induced kidney stained with Epo antibody. EPCs were visualized using HRP or immunofluorescent markers, highlighting perivascular Epo expression. Note Epo expression in previously identified EPCs (proximal tubules and peritubular interstitial fibroblasts; marked by asterisks), as well as by SMA^{+} perivascular cells (marked by arrows). **(A and B)** Epo-HRP immunostaining with eosin counterstaining. **(C–H)** Immunofluorescent Epo staining with the indicated cell type–specific markers: isolectin B4 (staining endothelial cells); CD73 (staining peritubular interstitial fibroblasts); SMA (staining pericytes and VSMC-like cells); LTL (staining distal tubules); and DBA (staining proximal tubules). Bar, 50 µm. Some images were cropped to more closely highlight Epo staining. Data are representative of at least two independent experiments (n = 3–5 animals per experiment).

erythropoiesis in noninduced control littermates. As a preliminary measure of active erythropoiesis, we measured the reticulocyte index at increasing VEGF plasma levels, demonstrating a dose-dependent increase in reticulocyte index in circulating blood with increasing VEGF (Fig. 7 A).

As a more direct erythropoietic readout, we quantified erythroblasts identified as cells double positive for the pan erythroid surface marker Ter119 and the nucleation marker DRAQ5 using FACS (Fig. 7 B). Because the spleen is also a potential erythropoietic site that in certain circumstances may substantially contribute to overall erythropoietic output by EME, we included both BM and spleen in this analysis. The total number of BM erythroblasts was found to be only moderately increased and only at the highest range of circulating VEGF levels (Fig. 7 C). In the spleen, however, the total erythroblast number was dramatically expanded with increasing VEGF level, with a nearly fourfold expansion taking place in the 700–1,000-pg/ml plasma VEGF range, thus bringing up the total erythroblast number to a significantly higher level than in control mice (Fig. 7 D). To directly visualize ongoing erythropoiesis, sections were triple immunostained with the erythroid lineage marker Ter119, the proliferation marker Ki67, and the nuclear stain DAPI for proliferating (triple positive) and nonproliferating (Ki67^{−}, double positive) erythroblasts. As shown in Fig. 7 (E and F) for spleen, VEGF elicited a robust splenic in situ erythroblast expansion.

To delineate steps in the erythropoietic cascade where VEGF-induced Epo may act, we examined the differentiation profile of erythroid progenitors in BM and spleen using the FACS-based assay described by Koulnis et al. (2011). In this procedure, the Ter119^{hi} cell population is further sorted according to size (forward scatter) and activation status (CD71 expression) and divided into EryA, EryB, and EryC erythroid progenitor subpopulations corresponding to the order of increased differentiation (Fig. 8 A). In both organs, a dose-dependent increase in VEGF-induced Epo plasma levels led to an increase in the relative frequency of early erythroid progenitors and, reciprocally, to a decrease in the relative frequency of late erythroid progenitors (see Fig. 8 B for a representative example and Fig. 8 C for quantification). These results indicate that the subpopulation of erythroid progenitors most expanded under VEGF is the EryA fraction, consisting mostly of basophilic erythroblasts, a fraction previously shown to be very responsive to Epo for its expansion (Vandekerckhove et al., 2009).

Discussion

This study introduces VEGF as a previously unrecognized inducer of Epo and perivascular Gli1^{+}SMA[+] PDGFRβ^{+} cells as a previously unrecognized reservoir of EPCs. It further shows that VEGF-induced Epo by this EPC subpopulation acts to increase
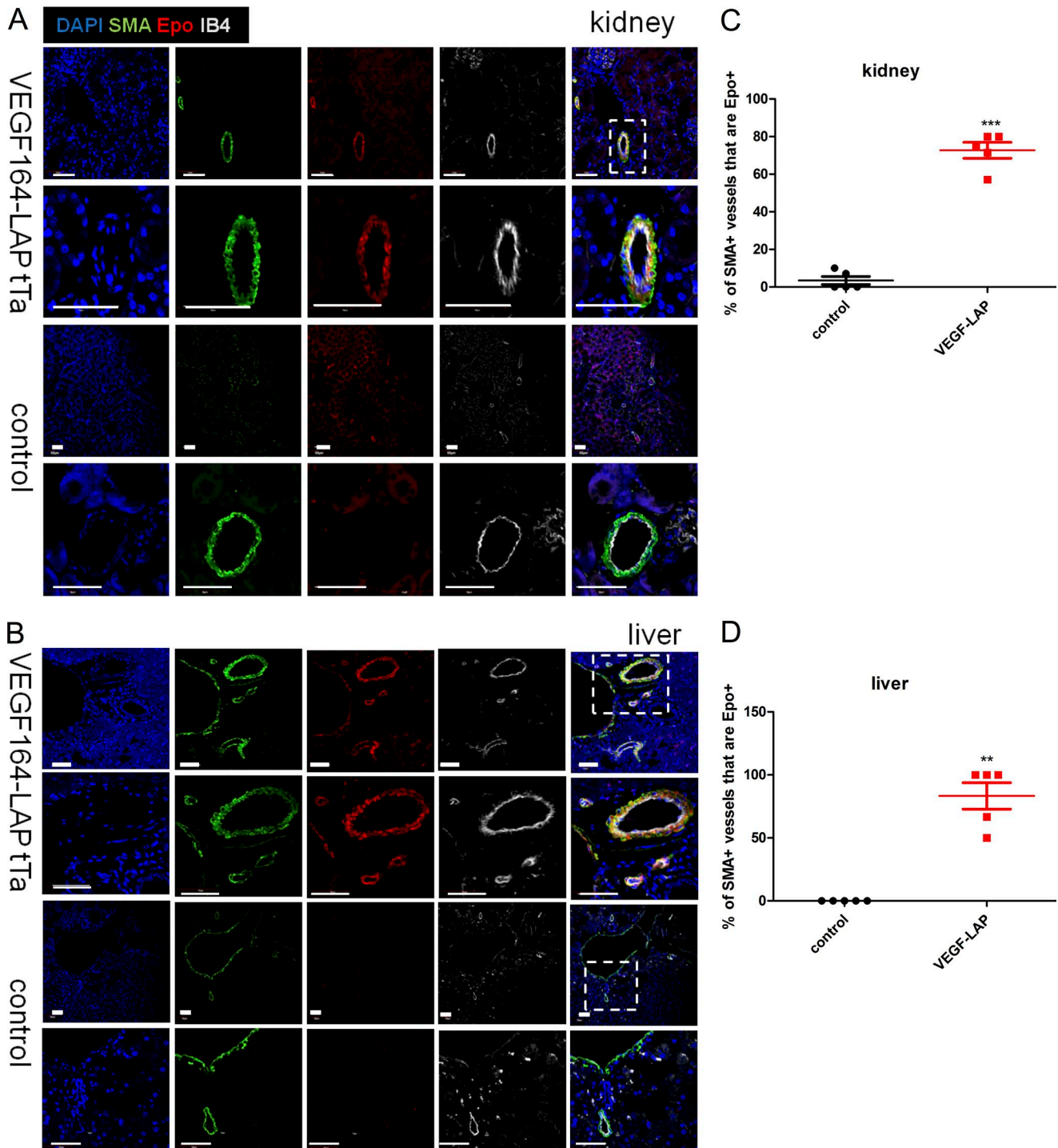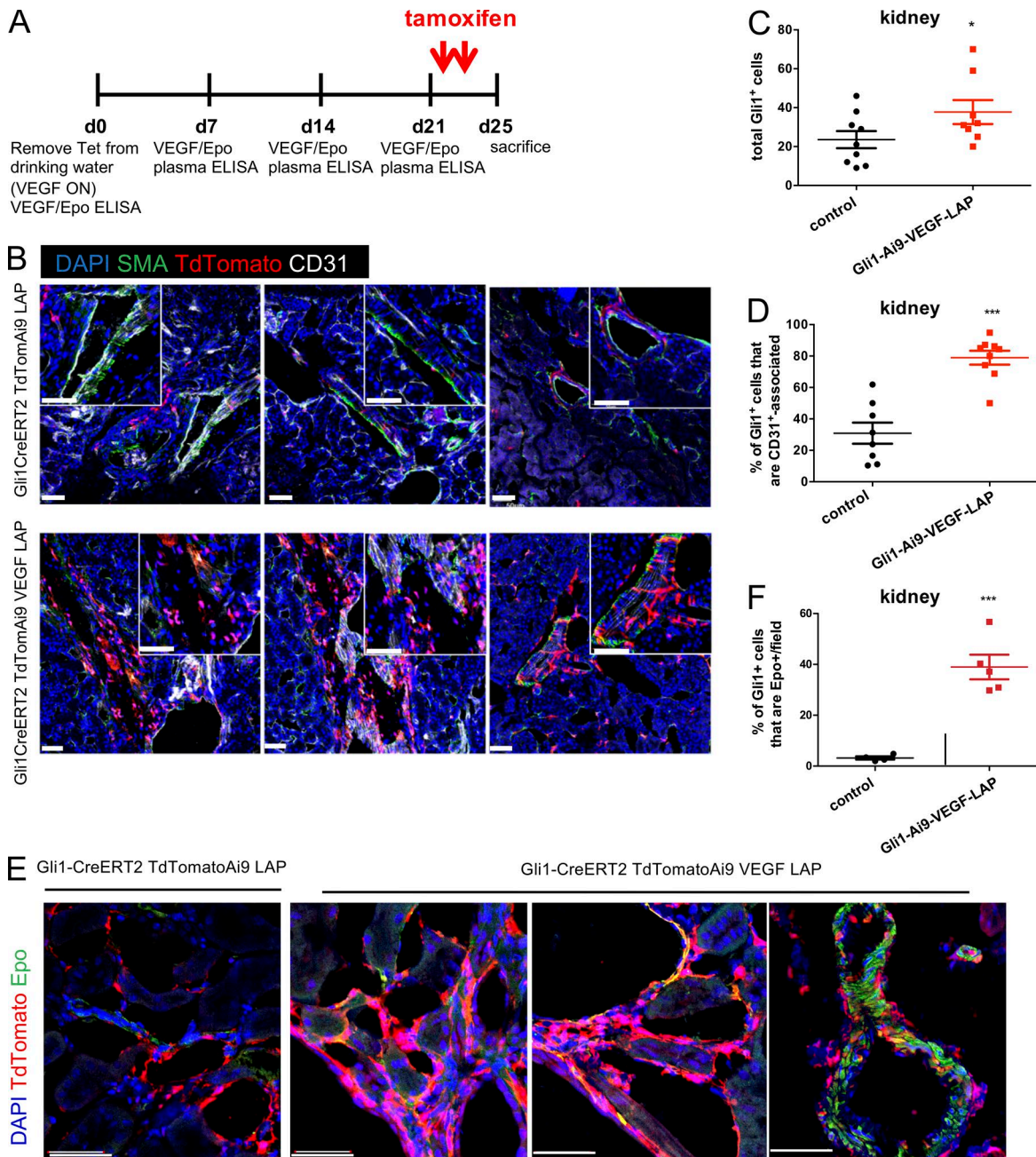
Figure 3. Epo expression by perivascular SMA+ cells in both kidney and liver is VEGF dependent. (A and B) Kidney (A) and liver (B) sections derived from VEGF-induced mice (TetVEGF164-LAPtTa) and control littermates (LAPtTa) were costained for Epo, SMA, IB4, and DAPI. Representative confocal images are shown at two magnifications each. Bar, 50 µm. The percentage of EPC-containing SMA+ vessels was determined per each genotype (*n* = 5 mice per group). Each data point represents the mean over five fields for each animal. Midline represents mean per group; error bars represent ±SEM. Data are representative of three independent experiments. **, P < 0.01; ***, P < 0.001 by unpaired two-tailed Student's *t* test.

erythropoietic output, the combined outcome of uncompromised BM erythropoiesis and induced splenic EME. The robust increase in plasma Epo induced by VEGF (>10-fold higher than physiological levels) results from its elevated production by three different organs: kidney, liver, and spleen. Normalized to

tissue mass, the kidney is clearly the organ most responsive to VEGF with respect to Epo up-regulation. Considering, however, the much larger size of the liver, the overall contribution of the latter to circulating Epo is also highly significant. VEGF induces Epo in a dose-dependent manner and is already evident at rela-

Greenwald et al.
VEGF expands erythropoiesis via Epo induction

Journal of Experimental Medicine
https://doi.org/10.1084/jem.20180752

220

Figure 4. **VEGF recruits alternative EPCs from Gli1⁺ perivascular MSC-like cells. (A)** Experimental scheme depicting Gli1 lineage tracing in Gli1-CreER::Ai9T-dTomato::Tet-VEGF164::LAP-tTA mice. VEGF was induced, and circulating VEGF and Epo levels were measured weekly by ELISA. A tamoxifen pulse was initiated after 3 wk of VEGF induction to stably label Gli1-expressing cells and their descendants with TdTomato. Triple transgenic mice missing the VEGF responder transgene served as littermate controls. **(B)** Representative confocal images of kidney sections derived from mice of the indicated genotype after Gli1 lineage tracing immunostained for TdTomato to highlight Gli1-expressing and descendant cells together with SMA and CD31 staining to examine a perivascular localization. Note a fraction of TdTomato⁺ cells also expressing SMA. **(C)** Quantification of Gli1⁺ cells based on immunostaining. Each data point represents 10 fields averaged over one animal (n = 7–8 mice per group). **(D)** Percentage of Gli1⁺ cells in contact with endothelial cells as determined by TdTomato/CD31 immunostaining. Each data point represents 10 fields averaged over one animal (n = 7–8 mice). **(E)** Representative confocal images obtained as described above and costained for TdTomato and Epo to highlight Epo-expressing Gli1-descendant cells, with Gli1-CreERT2 TdTomato-Ai9 LAP-tTa as the littermate control. Bar, 50 µm. **(F)** Percentage of Gli1⁺ cells that express Epo in kidney (n = 5–7 mice). Midline represents mean of each group; error bars represent ±SEM. *, $P < 0.05$; ***, $P < 0.001$, by unpaired two-tailed Student's t test. In B–F, results are representative of two independent experiments.

tively low doses of 200–400 pg/ml circulating VEGF, which are only two- to threefold higher than normal VEGF plasma levels. Notably, VEGF-induced Epo up-regulation in our experimental system takes place in the face of uncompromised erythropoiesis

and with no evidence of hypoxia or anemia, indicating that it is not a compensatory response to erythropoietic stress.

With regard to whether VEGF plays a role in homeostatic Epo production, it was previously shown that VEGF negatively regu-
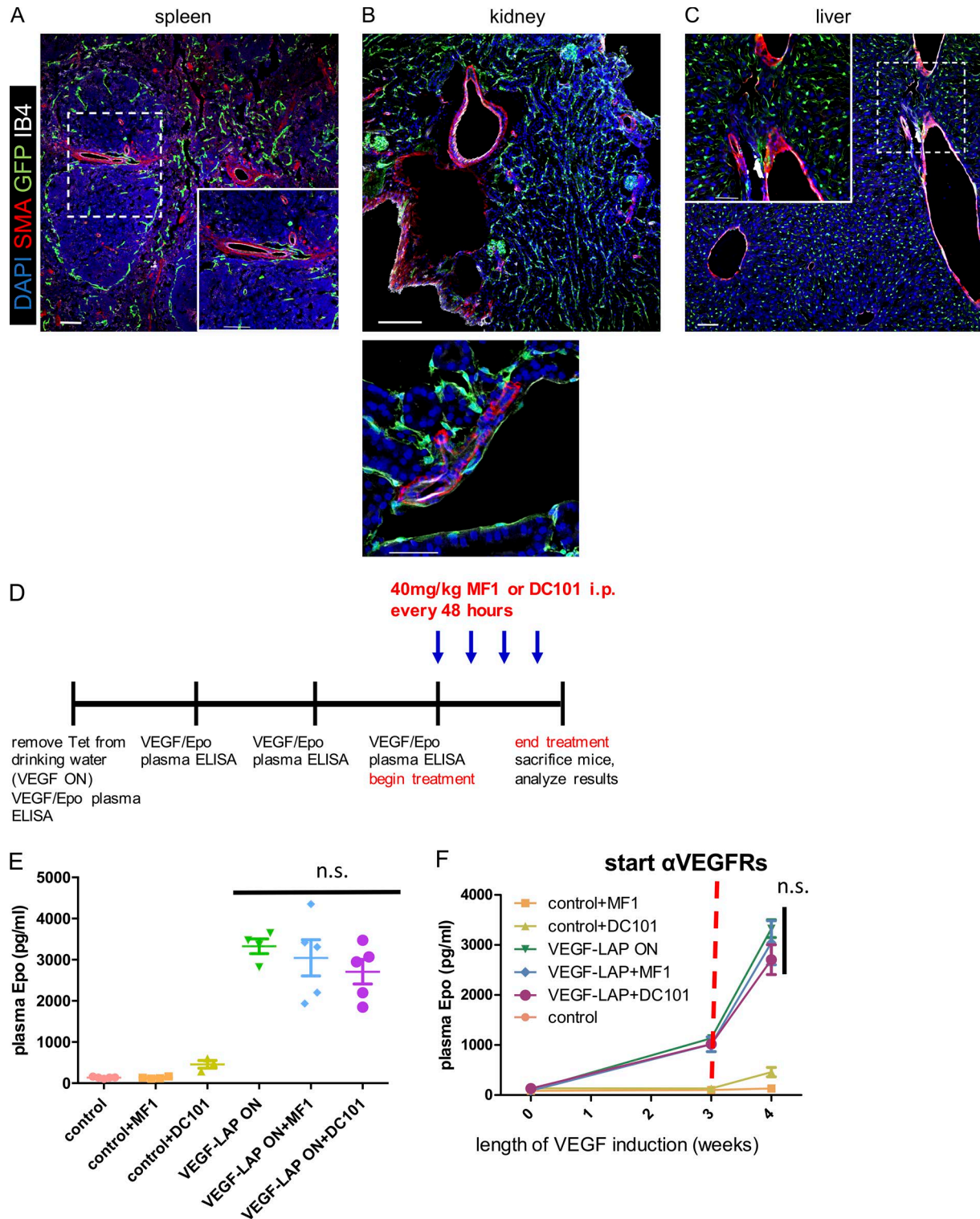
Figure 5. **Epo induction by VEGF is not mediated by canonical VEGF receptors. (A–C)** Immunostaining of spleen, kidney, and liver sections from VEGFR2-GFP knock-in mice. Note no VEGFR2 activity in SMA perivascular cells (i.e., in the cells that produce Epo under VEGF in the three organs). Results are representative of two independent experiments (n = 3 animals per experiment). Bar, 50 µm. **(D)** Scheme for VEGFR1 and VEGFR2 blockade using an i.p.-injected VEGFR1-neutralizing antibody (MF1), a VEGFR2-neutralizing antibody (DC101), or a vehicle PBS control. Reagents were injected at the indicated dose and schedule, starting 3 wk from VEGF induction and in age-matched controls (n = 4–5 animals per group). **(E and F)** Circulating Epo levels were monitored weekly from the onset of VEGF induction (E; n = 4–5 animals per group; midlines represent mean per group and error bars represent ±SEM) and at sacrifice (F; each data point represents the mean of 4–5 animals per group; error bars represent ±SEM). Results are representative of two independent experiments. n.s., P > 0.05, by unpaired two-tailed Student's t test in comparing treatment to control. n.s., not significant.
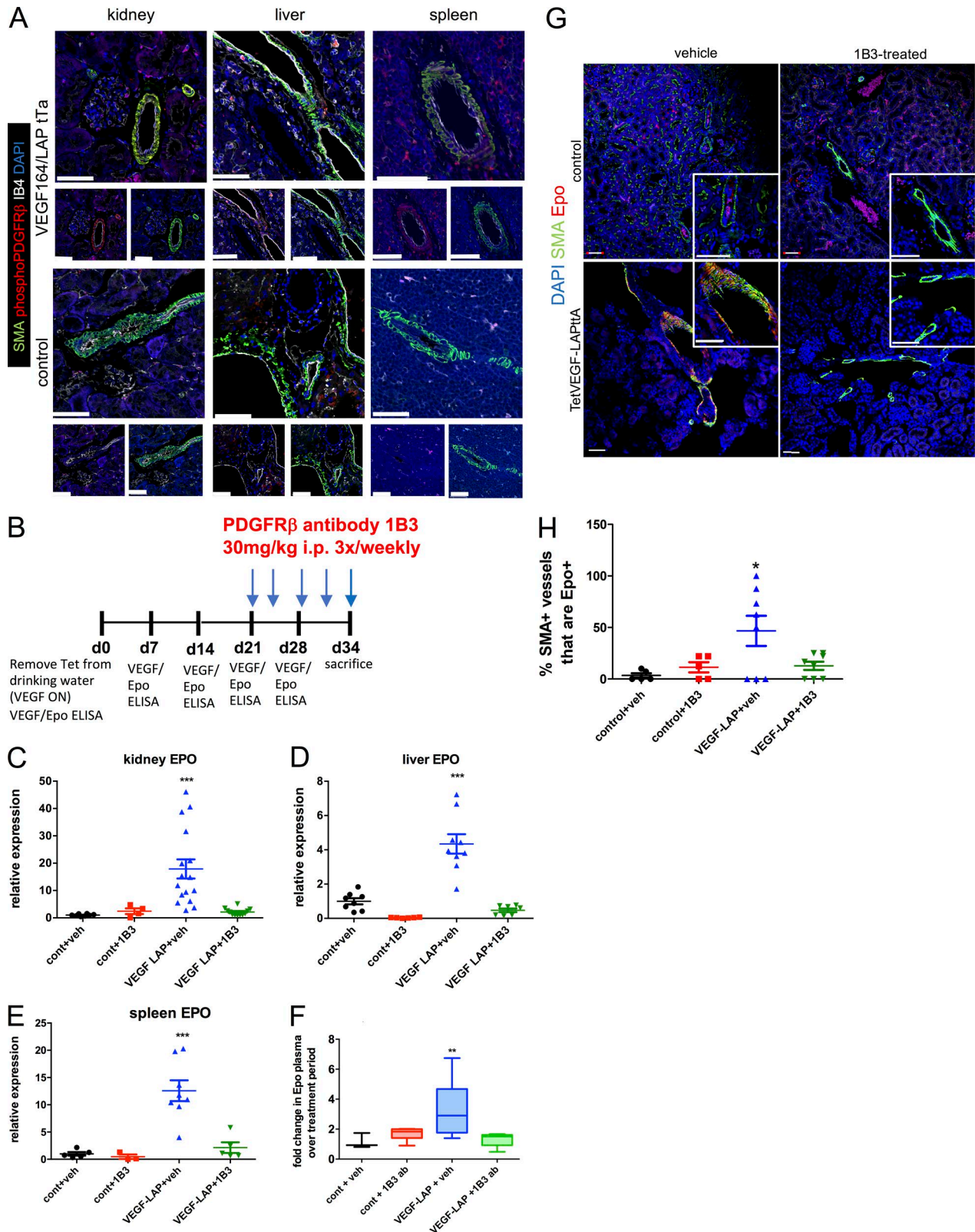
Figure 6. VEGF-induced perivascular Epo production is PDGFRβ dependent. (A) Representative confocal images of immunostaining of VEGF-induced (upper panels) and control (lower panels) kidney, liver, and spleen with the indicated markers from two independent experiments. To better visualize phosphorylated PDGFRβ in perivascular SMA⁺ cells, single staining is shown below the merged image. **(B)** Scheme of PDGFRβ blockade experiments using an i.p.-injected PDFGRβ-neutralizing antibody (1B3) or a vehicle PBS control. Reagents were injected at the indicated dose and schedule, starting 3 wk from VEGF induction and in age-matched controls (n = 5–9). **(C–E)** Relative gene expression for *Epo* normalized to GAPDH in the indicated organ at the end of the treatment period. Each data point represents a single animal, with the midline representing mean for the group and error bars representing ±SEM. **, P < 0.01; ***, P < 0.001, by one-way ANOVA with Tukey post-test. **(F)** Fold change in plasma Epo levels, with midlines representing the median for each group and error bars extending from

lates Epo synthesis by hepatocytes (but not by renal cells) using multiple VEGF inhibition strategies that increased hepatic Epo synthesis (Tam et al., 2006). On the contrary, we did not observe an increase in circulating Epo levels by systemic inhibition of VEGF using the VEGF trap Tet-sFlt1/LAP tTA mouse (Fig. S1). A possible explanation for this discrepancy is that some VEGF inhibition strategies (i.e., neutralization of VEGFR2 with DC101 mAb) may lead to a transient increase in circulating VEGF that could, in turn, induce Epo (Bocci et al., 2004). Additionally, Tam et al. (2006) focused on hepatocytes as Epo producers, whereas here VEGF was shown to regulate Epo in a perivascular EPC subpopulation in kidney, liver, and spleen. Interestingly, it was recently shown that the resultant hypoxia associated with some VEGF inhibition strategies may also induce renal Epo as an off-target effect (Nakamura et al., 2017), suggesting that Epo induction upon VEGF inhibition may be a function of the extent of resultant systemic hypoxia in any given VEGF inhibition strategy. Our results lead us to the conclusion that, while elevated VEGF at levels consistent with pathological conditions is clearly capable of augmenting nonhypoxic Epo production, it is dispensable for homeostatic Epo production.

Our findings on the EPC subpopulation engaged in VEGF-induced Epo production should be discussed with reference to known EPCs in other contexts. The identity of renal cells producing Epo under hypoxia based on in situ hybridization and immunostaining is somewhat controversial. A genetic labeling approach using Epo-GFP mice under anemia reinforced the notion that renal peritubular interstitial fibroblast-like cells of the cortex and outer medulla are the major producers of Epo under hypoxia, whereas the intercalated cells of the collecting ducts and proximal and distal tubules are the main producers of physiological Epo under normoxia (Pan et al., 2011; Nagai et al., 2014). It should be noted, however, that "peritubular interstitial fibroblast-like cells" is a broad term encompassing a heterogeneous group of renal interstitial cells that resemble fibroblasts and that the earlier confusion regarding the precise identity of renal EPCs is likely due to underappreciating the heterogeneity of this cellular pool. Consistent with this idea, it was recently shown that renal EPCs likely originate from a common FoxD1+ stromal progenitor capable of generating multiple subtypes of interstitial cells (Kobayashi et al., 2016). The range of cells capable of producing Epo under hypoxia was shown to also include astrocytes (Weidemann et al., 2009) and osteoblasts (Rankin et al., 2012).

With regard to EPCs under VEGF, we identified both classic EPCs as well as a unique population of SMA+ perivascular stromal cells resembling VSMCs (Fig. 5). The latter EPC subpopulation, we note, was not previously reported to produce Epo, unlike other stromal cell subpopulations that either produce Epo under hypoxia or can be manipulated pharmacologically by PHD2 inhibition to in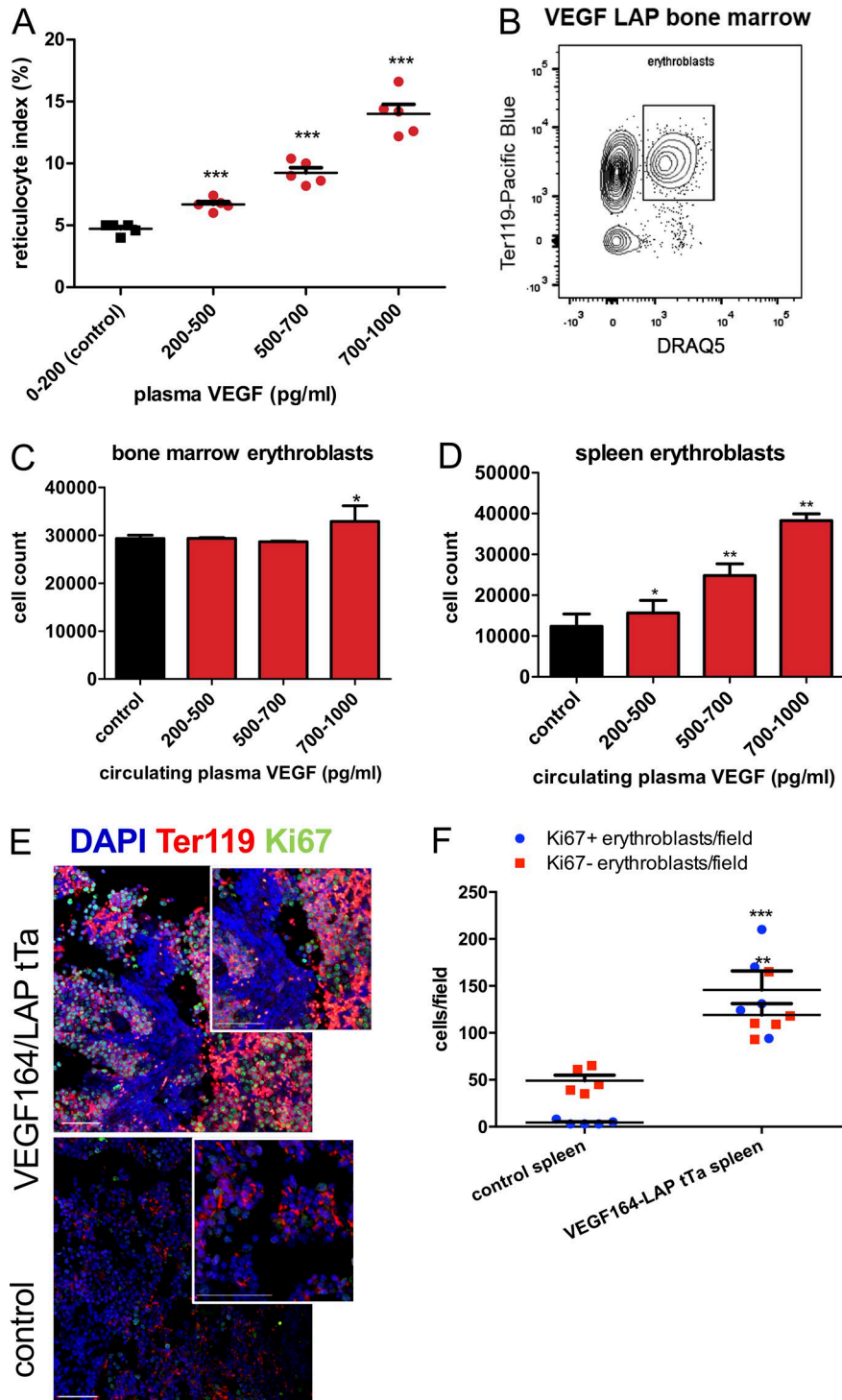duce Epo (Kobayashi et al., 2016). Considering that in all EPC subpopulations, VEGF induces Epo even under normoxia, in conjunction with findings that the total level of Epo production correlates with the EPC pool size (Obara et al., 2008; Koury and Haase, 2015), VEGF appears to be a highly efficient inducer of Epo production.

Using lineage tracing, we show that a significant fraction of Epo-expressing perivascular stromal cells under VEGF are descendants of Gli1+PDGFRβ+ MSC-like cells localized to the pericyte niche. Because recombination is not 100%, we speculate that the percentage of VEGF-induced EPCs that we identified as Gli1+ descendants is likely an underestimate. Notably, MSC-like progenitor cells may secrete factors contributing to a regenerative microenvironment upon organ injury (Caplan and Correa, 2011). On the other hand, Gli1+ cells have been shown to drive vascular calcification upon activation in CKD and contribute to injury-induced fibrosis (Kramann et al., 2015, 2016). In the face of CKD-associated fibrosis, Gli1+ cells expand and acquire SMA (Kramann et al., 2015). Interestingly, SMA acquisition is considered a hallmark of myofibroblast conversion associated with loss of ability to produce Epo by damaged renal EPCs (Asada et al., 2011; Kramann and Humphreys, 2014), although under VEGF, perivascular EPCs express SMA while retaining Epo-producing capability. In models of organ injury and subsequent angiogenesis, Gli1+ cells migrate from the adventitia into the medial layer and neointima and expand, acquiring a VSMC-like phenotype (Kramann et al., 2016). We observe a similar phenomenon upon VEGF induction, and we hypothesize that these cells are recruited to the EPC pool by VEGF.

Currently, there are ongoing efforts to prevent anemia development in CKD models through attempted restoration of Epo-producing capability in transformed SMA+ myofibroblasts or induction of alternate, ectopic cell populations to produce Epo (Bussolati et al., 2013; Kurt et al., 2015; Chang et al., 2016; Souma et al., 2016). For example, genetic inactivation of HIF prolyl hydroxylases in order to activate the HIF pathway has been used successfully to restore Epo production by SMA+ myofibroblast-transformed EPCs (Souma et al., 2016) and in recruiting both renin-expressing and mesangial cells to the EPC pool (Kurt et al., 2015). Our findings suggest another approach of compensation for an Epo deficit—namely, exploiting VEGF for the recruitment of perivascular Gli1+ SMA+PDGFRβ+ cells to the EPC pool.

Per the question of how VEGF interacts with perivascular SMA+Gli1+PDGFRβ+ cells, previous studies have shown that VEGF may promote an association between endothelial cells and Gli1+ cells (Kramann et al., 2015), that VEGF can regulate MSC mobilization and recruitment to sites of neovascularization, and that VEGF signaling to MSCs devoid of VEGFRs is mediated by PDGF receptors via direct tyrosine phosphorylation induced by VEGF (Ball et al., 2007). These findings are consistent with our observation that VEGF-induced Epo up-regulation in Gli1+

the first quartile to the minimum and from the third quartile to the maximum values. **, P < 0.01 by one-way ANOVA with Tukey post-test. **(G)** Confocal images of kidney sections treated with PDGFRβ-neutralizing antibody 1B3 (or vehicle control) and immunostained with the indicated markers. Higher magnification shown in insets; bars, 50 µm. **(H)** Percentage of SMA-surrounded kidney vessels containing Epo-expressing cells calculated on the basis of images such as the one shown in G. Each data point represents the average for multiple vessels of a single animal. Error bars represent ±SEM. *, P < 0.05 by one-way ANOVA with Tukey post-test. Results are representative of two independent experiments.

Greenwald et al.
VEGF expands erythropoiesis via Epo induction

Journal of Experimental Medicine
https://doi.org/10.1084/jem.20180752

224

Figure 7. VEGF boosts erythropoiesis in both BM and spleen through expansion of the erythroid progenitor pool. (A) Reticulocyte index in the blood of VEGF-induced mice at increasing circulating VEGF levels ($n = 5$ mice per VEGF range, two independent repeats). Error bars represent ±SEM. ***, $P < 0.001$ compared with control by one-way ANOVA. **(B–D)** FACS-aided quantification of erythroblasts defined as cells double positive for Ter119 and the nuclear marker DRAQ5 (B) in BM (C) and spleen (D; $n = 5$ per each VEGF plasma range). *, $P < 0.05$; **, $P < 0.01$ by unpaired two-tailed Student's t test in which each VEGF range was compared against control. Results were combined from three independent experiments. **(E and F)** Immunostaining of proliferating erythroblasts in spleen of VEGF-induced mice and control littermates (E) and enumeration of proliferating (DAPI$^+$/Ter119$^+$/Ki67$^+$) versus nonproliferating (DAPI$^+$/Ter119$^+$Ki67$^-$) erythroblasts based on immunostaining (F; $n = 5$ per group). Bar, 50 µm. Each data point represents the mean averaged over five fields per animal. Error bars represent ±SEM, and midline represents mean of the group. Results are representative of two independent experiments. **, $P < 0.01$; ***, $P < 0.001$ by unpaired two-tailed Student's t test.

SMA$^+$PDGFRβ$^+$ cells is not mediated by the canonical VEGF receptors but rather by PDGFRβ. This finding is also consistent with a study using tumor-bearing mice showing that tumor-derived PDGF-BB signaling via PDGFRβ can activate the *Epo* promoter and induce ectopic Epo production in spleen stromal cells under normoxia (Xue et al., 2011). While our results clearly show that PDGFRβ is indispensable for VEGF-induced recruitment of this particular EPC population and hint at a direct mode of action, the possibility that VEGF indirectly signals to PDGFRβ via up-regulation of PDGF-BB, the canonical PDGFRβ ligand, should be

examined and cannot be ruled out. Interestingly, PDGFRβ was shown to negatively regulate ectopic erythropoiesis in the placental labyrinth vasculature vis-à-vis Epo production by placental trophoblasts, demonstrating multiple roles for PDGFRβ in Epo regulation that are context dependent (Chhabra et al., 2012).

We have shown that robust erythropoiesis can be established outside the BM merely by increasing circulating VEGF levels within a permissive range (300–1,000 pg/ml). Remarkably, VEGF-induced EME boosts overall erythropoietic output because, unlike stress-induced EME, it is not at the expense of compro-
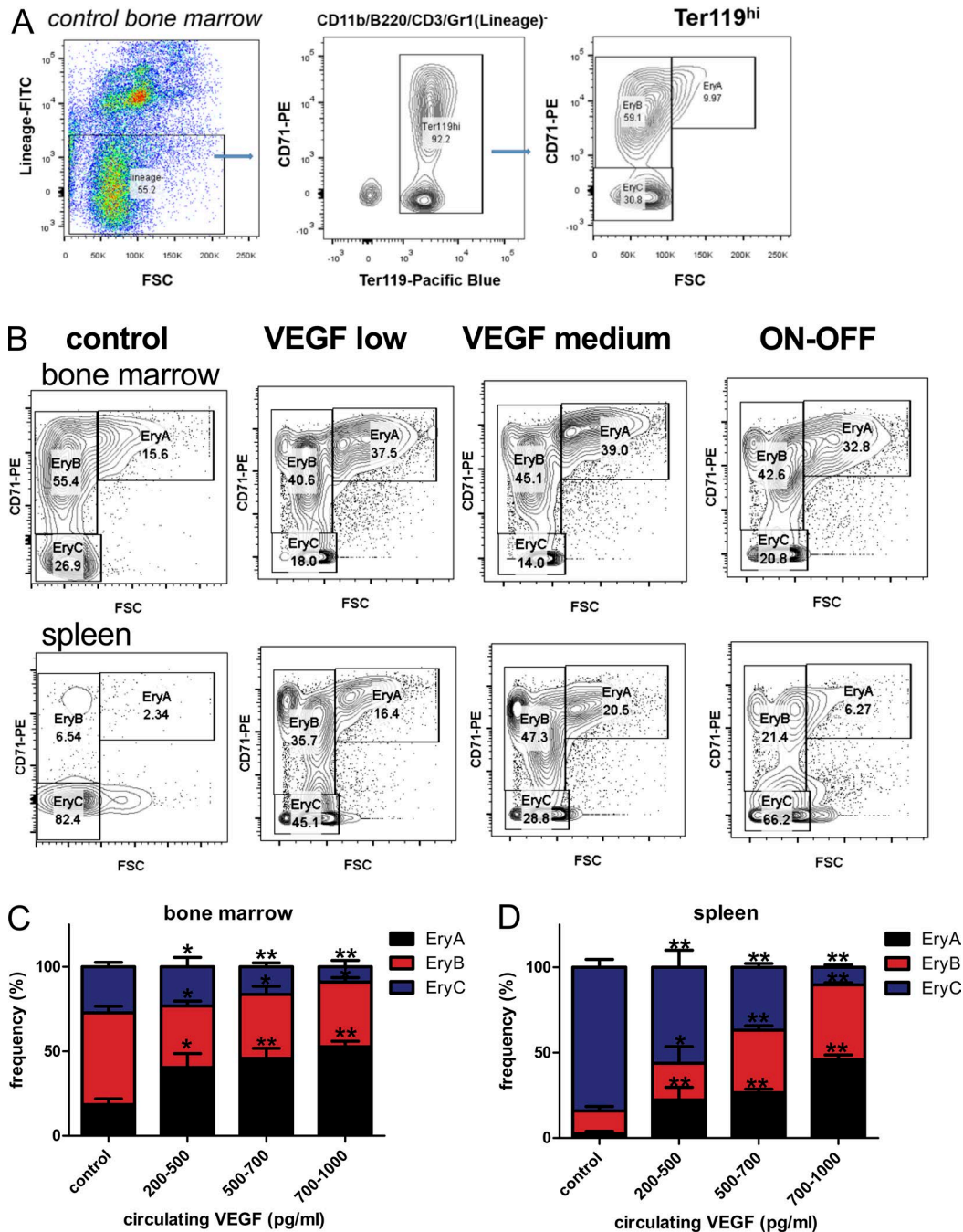
Greenwald et al.
VEGF expands erythropoiesis via Epo induction

Journal of Experimental Medicine
https://doi.org/10.1084/jem.20180752

225

Figure 8. **VEGF-induced Epo promotes early to intermediate erythroblast differentiation. (A)** FACS analysis for assessing erythroid progenitor differentiation. After exclusion of cells positive for other lineages, the Ter119hi population is gated to identify erythroid progenitors. Forward scatter (FSC) and CD71 expression of the Ter119hiLin- population subdivides erythroid progenitors according to their differentiation status into EryA (basophilic erythroblasts), EryB (late basophilic erythroblasts), and EryC (orthochromatic erythroblasts/reticulocytes). **(B)** Representative FACS density plots of erythroid progenitor subsets at increasing VEGF levels and in VEGF ON–OFF in BM (upper panel) and spleen (lower panel). **(C and D)** BM (C) and spleen (D) erythroid progenitor subset frequencies were enumerated at increasing circulating VEGF levels (n = 5–9 animals per group). Results were combined from three independent experiments. *, P < 0.05; **, P < 0.01 by unpaired two-tailed Student's t test in which each VEGF range was compared with control. Error bars represent SEM.

mised BM erythropoiesis and occurs under normoxic conditions. Our observation that EME is VEGF dose dependent, with a differentiation defect resulting in ineffective erythropoiesis taking place at excessively high levels of circulating VEGF (≥1,200 pg/ml) for an extended period of time (data not shown), may explain the discrepancy of why, in some contexts, VEGF overexpression has been reported to result in enhanced erythropoiesis (Cerdan

et al., 2004; Cervi et al., 2007; Xue et al., 2009; Rehn et al., 2014), whereas in other circumstances, an erythroid differentiation defect resulting in anemia was observed (Drogat et al., 2010). We speculate that when circulating VEGF levels are between 300 and 1,000 pg/ml in pathological scenarios, as seen in many cancers (Kraft et al., 1999), VEGF may augment erythropoiesis, but that at VEGF levels exceeding this threshold, which is often observed

Greenwald et al.
VEGF expands erythropoiesis via Epo induction

Journal of Experimental Medicine
https://doi.org/10.1084/jem.20180752

226

in advanced metastatic disease, elevated VEGF may contribute to anemia (Salven et al., 1997). Likewise, our findings may explain the correlation reported in the clinical literature between VEGF serum levels, EME, and ineffective erythropoiesis (Panteli et al., 2007; Maktouf et al., 2011; Prakash et al., 2012).

Recombinant Epo has been used extensively to treat anemia, but its use in anemic cancer patients remains controversial. While administration of recombinant Epo has been shown to ameliorate anemia, disease progression and long-term survival rates worsen when patients with metastatic cancer are treated with Epo (Leyland-Jones et al., 2005; Spivak, 2005), raising concerns that Epo is protumorigenic and proangiogenic. Our finding that elevated VEGF induces Epo raises the possibility that VEGF-Epo cross-talk may have an amplifying role in cancer cell proliferation and tumor angiogenesis in hypoxic tumors in which VEGF and Epo are coinduced. There are also circumstances other than tissue hypoxia where VEGF might augment Epo. For example, we suspect that hormonally induced VEGF in pregnancy might play a role in an apparent transient increase in splenic EME.

Erythropoiesis is a complex multistep process in which Epo plays a fundamental early role. Our analysis of erythroid differentiation reveals that VEGF indeed acts to preferentially expand basophilic erythroblasts, an erythroid progenitor subpopulation highly responsive to Epo. Yet, explaining how VEGF as a singly induced factor can drive all subprocesses of productive EME—including HSC mobilization, extramedullary retention, creation of a proper erythropoietic niche, and provision of complementary erythropoietic factors—is currently poorly understood and is the subject of ongoing study in our laboratory.

Materials and methods

Animals

Elevated levels of circulating VEGF164 were achieved through liver-specific VEGF overexpression by using a driver line in which tet-regulated transactivator (tTA) expression is driven by a C/EBPβ (CCAAT/enhancer-binding protein β) promoter (also known as liver-activator protein). The responder tet-VEGF164 transgenic line was previously described (Dor et al., 2002). The responder tet-VEGF TRAP (soluble fms-like tyrosine kinase [sFlt]) transgenic line encodes a tetracycline-inducible protein composed of an IgG1-Fc tail fused to the extracellular domain of VEGF-R1/sFlt (corresponding to amino acid residues 1–631 in human VEGF-R1/sFlt; described in May et al., 2011). For maintaining VEGF or sFlt1 in the OFF state, drinking water was supplemented with 500 mg/liter tetracycline (Tevacycline; Teva) and 3% sucrose. Induction of VEGF or sFlt1 was performed by replacing tetracycline-supplemented water with fresh water. VEGF or sFlt could be subsequently shut off (ON–OFF) by reintroduction of tetracycline to the drinking water. Animals harboring LAP tTa alone served as controls unless noted otherwise.

Flk-1$^{GFP/+}$ mice in which GFP is targeted to the VEGFR2 (Flk-1) gene locus were used to evaluate Flk1 expression on SMA⁺ perivascular stromal cells in kidney, liver, and spleen (provided by A. Medvinsky, Institute for Stem Cell Research, University of Edinburgh, Scotland, UK). Gli1-CreERT2;Ai9 TdTomato/Tet VEGF164-LAP tTa mice were generated from Gli1-CreERT2 mice from The Jackson Laboratory (JAX 007913) crossed with an Ai9-tdTomato reporter line (The Jackson Laboratory; JAX 007909), Tet VEGF164, and LAP tTa. Tamoxifen was prepared in sunflower seed oil (Sigma)/ethanol and administered orally once daily for 3 d. Controls were Gli1-CrERT2:Ai9 TdTomato LAP tTa littermates that lacked the VEGF164 transgene. Due to the need to cross multiple genetic strains, mice are of mixed C57BL6-ICR backgrounds.

ELISA

The following commercially available ELISA kits were used to measure protein levels in plasma and tissue lysates: mouse VEGF Quantikine ELISA kit (R&D Systems; MV00), human sFlt Quantikine ELISA kit (R&D Systems; DVR100B), and mouse Epo Quantikine ELISA kit (R&D Systems; MEP00). Blood for plasma collection was drawn via the tail vein with 12 mM EDTA or heparin as an anticoagulant and then centrifuged for 20 min at 2,000 *g*. Tissue lysates for ELISA were homogenized in PBS using a Next Advance Bullet Blender homogenizer, stored overnight at –20°C, and lysed with two freeze–thaw cycles followed by centrifugation for 5 min at 5,000 *g* and collection of the supernatant. The Bradford assay was performed to standardize tissue lysate concentrations according to the manufacturer's instructions (Bio-Rad Protein Assay Dye Reagent Concentrate; 500-0006). ELISAs were read at 450 nm with a reference value of 540 nm using a Tecan Infinite f200 Pro 96-well plate reader.

FACS

A single-cell suspension was prepared from BM following aspiration from the femur and tibia with a 26-gauge syringe and PBS. A single-cell suspension was prepared from spleen following mechanical dissociation and filtration through a 40-μm cell filtration cap. Single-cell suspensions were washed in staining buffer (0.2% BSA and 5 mM glucose in PBS), and 2 × 10⁶ cells per sample were resuspended in the staining buffer for staining with the following anti-mouse antibodies. Lineage exclusion cocktail (all antibodies used at 1:400): FITC rat anti-mouse CD41 (BioLegend; 133904), FITC rat anti-mouse CD45R/B220 (BioLegend; 103206), FITC rat anti-mouse CD3 (BioLegend; 10024), FITC rat anti-mouse CD11b (BioLegend; 101206), and FITC rat anti-mouse Gr-1 (BioLegend; 108406). Erythroid markers: FITC rat anti-mouse Ter119 1:200 (BioLegend; 116206), Pacific Blue rat anti-mouse Ter119 1:200 (BioLegend; 116232), biotin rat anti-mouse Ter119 1:200 (BioLegend; 116203), PE rat anti-mouse CD71 PE 1:200 (eBioscience; clone R17217), and DRAQ5 1:500 (eBioscience; 65-0880). Secondary antibody: strepavidin-APC-Cy7 (BioLegend;, 405208). FACS was performed on a MACS Quant Analyzer (Miltenyi), and FACS analysis was completed on FlowJo version 10.

RNA isolation

Tissues for RNA isolation were homogenized using a Next Advance Bullet Blender homogenizer. RNA was isolated using Tri-Reagent (Sigma) according to the manufacturer's instructions. RNA was quantified using a Nanodrop spectrophotometer.

Greenwald et al.
VEGF expands erythropoiesis via Epo induction

Journal of Experimental Medicine
https://doi.org/10.1084/jem.20180752

227

cDNA preparation

cDNA was prepared from RNA using a high-capacity cDNA reverse transcription kit with RNase inhibitor (Applied Biosystems) according to the manufacturer's instructions.

qPCR primers

Primers were designed by using Primer Express (Applied Biosystems) and the National Center for Biotechnology Information's PrimerBlast. Primers were synthesized by Sigma Israel or Integrated DNA Technologies. The sequences for the primers used were as follows: GAPDH-s: 5′-CCTGGAGAAACCTGCCAAG-3′; GAPDH-as: 5′-CAACCTGGTCCTCAGTGTAGC-3′; EPO-s: 5′-AATGGAGGTGGAAGAACAGGCCAT-3′; EPO-as: 5′-CGAAGCAGTGAAGTGAGGCTACGTA-3′; Glut1-s: 5′-CAAGGACACACTAATACCGAAC-3′, Glut1-as: 5′-TAGGAAGAGACAGGAATGGGCGAA-3′; Pgk-s: 5′-CGCTGTTCTCCTCTTCCTCATCT-3′; Pgk-as: 5′-TCATCACGACCCGCTTCCC-3′; LdhA-s: 5′-GGTGTTGAGATGGTGTGGG-3′; and LdhA-as: 5′-GCAGTTGGCAGTGTGTC-3′.

Quantitative real-time PCR (qPCR)

FAST SYBR Green Master Mix (Applied Biosystems) was used for qPCR according to the manufacturer's instructions. Real-time PCR was performed on an Applied Biosystems StepOne Plus qPCR machine. An extra dissociation step was added. qPCR results were analyzed using StepOne Plus Software v2.3 (Applied Biosystems). Expression of all genes was normalized to GAPDH.

Hematological analysis

Blood for complete blood counts was drawn via tail vein and collected into micro-EDTA–coated collection tubes (BD; K2E microtainers) and then analyzed by a Mindray BC-2800 Vet hematology analyzer.

Immunohistochemistry

5-μm paraffin sections were cut from liver, spleen, and kidney. Antigen retrieval was performed by citrate buffer (pH 6; Zymed Laboratories) in a pressure cooker. Frozen sections were prepared by fixation in 4% paraformaldehyde followed by treatment in 30% sucrose and embedded in optimal cutting temperature compound before cutting 10–12-μm sections on a Leica CM1950 cryostat.

Immunofluorescence was performed by using both paraffin and frozen sections of VEGF-LAP and control liver, spleen, and kidney. Sections were blocked in 1% BSA and 0.5% Triton X-100. Primary antibodies included rabbit Epo antibody (1:50, H-162, sc-7956; Santa Cruz), mouse Epo antibody (1:50, 7D10, sc-80995; Santa Cruz), rabbit SMA (1:200, ab32575; Abcam), mouse SMA (1:200, ab7817; Abcam), rabbit phospho-PDGFRβ (1:50, phospho Y1021, ab62437; Abcam), rabbit GFP (1:200, G10362; Invitrogen), mouse CD68 (1:200, KP1, ab955; Abcam), rat CD73 (1:50, 14-0731; eBioscience), rat Ter119 (1:100, ab91113; Abcam), rabbit Ki67 (1:200, SP6, RM9106S; Thermo Scientific), rat PDGFRβ (1:00, 14-1402, APB5; eBioscience), and rabbit VCAM1 (1:50, EPR5047, ab134047; Abcam). Lectins and dyes included DRAQ5 (1:1,000, 65-0880-92; eBioscience), biotinylated GSLI-isolectin B4 (1:10, B-1205; Vector Laboratories), DBA rhodamine (1:100, RL-1032; Vector Laboratories), and LTL fluorescein (1:100, FL-1321; Vec-

tor Laboratories). Sections were incubated in primary antibody overnight and diluted in 1% BSA and 0.5% Triton X-100 at 4°C. Pimonidazole (60 mg/kg Hypoxyprobe; Chemicon) was injected i.p. 30 min before the animals were sacrificed. Fluorescent secondary antibodies included donkey anti-mouse, rabbit, and rat conjugated to AF488, AF647, Cy3, and extravidin (The Jackson Laboratory) used at 1:200. Sections were mounted with Permafluor mounting medium containing DAPI (Thermo Fisher Scientific). Confocal microscopy was performed using an Olympus FV-1000 using the 20×, 40×, and 80× objectives with single-plane or Z-stack acquisition. Confocal images were analyzed with FV10-ASW 3.0 Viewer and ImageJ (National Institutes of Health).

In vivo inhibition with Flt1/VEGFR1 and Flk1/VEGFR2 neutralizing antibodies

MF1, a monoclonal neutralizing antibody against Flt1/VEGFR1, and DC101, a monoclonal neutralizing antibody against Flk1/VEGFR2 (both gifts from Eli Lilly & Co.) were injected i.p. at a dose of 40 mg/kg 3×/wk for a period of 1 wk in Tet VEGF164/LAP tTa mice that had been overexpressing VEGF for a period of 3 wk at the initiation of the experiment and control monotransgenic LAP tTa mice. Circulating VEGF and Epo levels were evaluated in response to the treatment.

In vivo inhibition with PDGFRβ-neutralizing antibody

PDGFRβ-neutralizing antibody (1B3, provided by Eli Lilly & Co.) was administered i.p. 3×/wk at a dose of 30 mg/kg for 2 wk to TetVEGF164-LAPtTa mice following 3 wk of VEGF induction and to a group of control (LAPtTa) mice over the same period. Additionally, vehicle (saline) was administered to matched groups of VEGF-induced mice and control mice over the same treatment period (n = 5–9 animals per group).

Statistical analysis

For comparison between two groups, Student's t test was used, and P values assumed two-tailed distribution and unequal variances (*, $P < 0.05$; **, $P < 0.01$; ***, $P < 0.001$). Comparisons between multiple groups were calculated by one-way ANOVA with Tukey post-test. Statistical information relevant to individual experiments is detailed in the figure legends. GraphPad Prism 7 software was used for statistical analysis. For animal studies, the investigator was not blinded during group allocation, the experiment, or when assessing the outcome.

Study approval

Animal experiments were performed in accordance with Hebrew University of Jerusalem Institutional Animal Care and Use Committee guidelines under animal ethics protocols MD-13-13939-2 and MD-17-15101-4.

Online supplemental material

Fig. S1 shows the effect of VEGF inhibition (by sFlt overexpression) on homeostatic Epo production by ELISA, qPCR, and blood smear. Fig. S2 shows Epo expression under VEGF induction in spleen by immunostaining. Fig. S3 shows immunostaining for phosphorylated PDGFRβ following VEGF induction and de-induction.

References

Asada, N., M. Takase, J. Nakamura, A. Oguchi, M. Asada, N. Suzuki, K. Yamamura, N. Nagoshi, S. Shibata, T.N. Rao, et al. 2011. Dysfunction of fibroblasts of extrarenal origin underlies renal fibrosis and renal anemia in mice. *J. Clin. Invest.* 121:3981–3990. https://doi.org/10.1172/JCI57301

Baccarani, M., A. Zaccaria, G.P. Bagnara, M.A. Santucci, M.A. Brunelli, and S. Tura. 1978. The relevance of extramedullary hemopoiesis to the staging of chronic myeloid leukemia. *Boll. Ist. Sieroter. Milan.* 57:257–270.

Ball, S.G., C.A. Shuttleworth, and C.M. Kielty. 2007. Vascular endothelial growth factor can signal through platelet-derived growth factor receptors. *J. Cell Biol.* 177:489–500. https://doi.org/10.1083/jcb.200608093

Bautz, F., S. Rafii, L. Kanz, and R. Möhle. 2000. Expression and secretion of vascular endothelial growth factor-A by cytokine-stimulated hematopoietic progenitor cells. Possible role in the hematopoietic microenvironment. *Exp. Hematol.* 28:700–706. https://doi.org/10.1016/S0301-472X(00)00168-5

Bocci, G., S. Man, S.K. Green, G. Francia, J.M.L. Ebos, J.M. du Manoir, A. Weinerman, U. Emmenegger, L. Ma, P. Thorpe, et al. 2004. Increased plasma vascular endothelial growth factor (VEGF) as a surrogate marker for optimal therapeutic dosing of VEGF receptor-2 monoclonal antibodies. *Cancer Res.* 64:6616–6625. https://doi.org/10.1158/0008-5472.CAN-04-0401

Bussolati, B., C. Lauritano, A. Moggio, F. Collino, M. Mazzone, and G. Camussi. 2013. Renal CD133(+)/CD73(+) progenitors produce erythropoietin under hypoxia and prolyl hydroxylase inhibition. *J. Am. Soc. Nephrol.* 24:1234–1241. https://doi.org/10.1681/ASN.2012080772

Caplan, A.I., and D. Correa. 2011. The MSC: an injury drugstore. *Cell Stem Cell.* 9:11–15. https://doi.org/10.1016/j.stem.2011.06.008

Cerdan, C., A. Rouleau, and M. Bhatia. 2004. VEGF-A165 augments erythropoietic development from human embryonic stem cells. *Blood.* 103:2504–2512. https://doi.org/10.1182/blood-2003-07-2563

Cervi, D., Y. Shaked, M. Haeri, T. Usenko, C.R. Lee, J.J. Haigh, A. Nagy, R.S. Kerbel, E. Yefenof, and Y. Ben-David. 2007. Enhanced natural-killer cell and erythropoietic activities in VEGF-A–overexpressing mice delay F-MuLV-induced erythroleukemia. *Blood.* 109:2139–2146. https://doi.org/10.1182/blood-2005-11-026823

Chang, Y.-T., C.-C. Yang, S.-Y. Pan, Y.-H. Chou, F.-C. Chang, C.-F. Lai, M.-H. Tsai, H.-L. Hsu, C.-H. Lin, W.-C. Chiang, et al. 2016. DNA methyltransferase inhibition restores erythropoietin production in fibrotic murine kidneys. *J. Clin. Invest.* 126:721–731. https://doi.org/10.1172/JCI82819

Chhabra, A., A.J. Lechner, M. Ueno, A. Acharya, B. Van Handel, Y. Wang, M.L. Iruela-Arispe, M.D. Tallquist, and H.K.A. Mikkola. 2012. Trophoblasts regulate the placental hematopoietic niche through PDGF-B signaling. *Dev. Cell.* 22:651–659. https://doi.org/10.1016/j.devcel.2011.12.022

Choi, S.H., D. Ruggiero, R. Sorice, C. Song, T. Nutile, A. Vernon Smith, M.P. Concas, M. Traglia, C. Barbieri, N.C. Ndiaye, et al. 2016. Six Novel Loci Associated with Circulating VEGF Levels Identified by a Meta-analysis of Genome-Wide Association Studies. *PLoS Genet.* 12:e1005874. https://doi.org/10.1371/journal.pgen.1005874

Dor, Y., V. Djonov, R. Abramovitch, A. Itin, G.I. Fishman, P. Carmeliet, G. Goelman, and E. Keshet. 2002. Conditional switching of VEGF provides new insights into adult neovascularization and pro-angiogenic therapy. *EMBO J.* 21:1939–1947. https://doi.org/10.1093/emboj/21.8.1939

Drogat, B., J. Kalucka, L. Gutiérrez, H. Hammad, S. Goossens, M. Farhang Ghahremani, S. Bartunkova, K. Haigh, K. Deswarte, O. Nyabi, et al. 2010. Vegf regulates embryonic erythroid development through Gata1 modulation. *Blood.* 116:2141–2151. https://doi.org/10.1182/blood-2010-01-264143

Feng, C.C., G.X. Ding, N.H. Song, X. Li, Z. Wu, H.W. Jiang, and Q. Ding. 2013. Paraneoplastic hormones: parathyroid hormone-related protein (PTHrP) and erythropoietin (EPO) are related to vascular endothelial growth factor (VEGF) expression in clear cell renal cell carcinoma. *Tumour Biol.* 34:3471–3476. https://doi.org/10.1007/s13277-013-0924-7

Forsythe, J.A., B.H. Jiang, N.V. Iyer, F. Agani, S.W. Leung, R.D. Koos, and G.L. Semenza. 1996. Activation of vascular endothelial growth factor gene transcription by hypoxia-inducible factor 1. *Mol. Cell. Biol.* 16:4604–4613. https://doi.org/10.1128/MCB.16.9.4604

Gerber, H.-P., A.K. Malik, G.P. Solar, D. Sherman, X.H. Liang, G. Meng, K. Hong, J.C. Marsters, and N. Ferrara. 2002. VEGF regulates haematopoietic stem cell survival by an internal autocrine loop mechanism. *Nature.* 417:954–958. https://doi.org/10.1038/nature00821

Grover, A., E. Mancini, S. Moore, A.J. Mead, D. Atkinson, K.D. Rasmussen, D. O'Carroll, S.E.W. Jacobsen, and C. Nerlov. 2014. Erythropoietin guides multipotent hematopoietic progenitor cells toward an erythroid fate. *J. Exp. Med.* 211:181–188. https://doi.org/10.1084/jem.20131189

Hattori, K., S. Dias, B. Heissig, N.R. Hackett, D. Lyden, M. Tateno, D.J. Hicklin, Z. Zhu, L. Witte, R.G. Crystal, et al. 2001. Vascular endothelial growth factor and angiopoietin-1 stimulate postnatal hematopoiesis by recruitment of vasculogenic and hematopoietic stem cells. *J. Exp. Med.* 193:1005–1014. https://doi.org/10.1084/jem.193.9.1005

Huang, Y., X. Chen, M.M. Dikov, S.V. Novitskiy, C.A. Mosse, L. Yang, and D.P. Carbone. 2007. Distinct roles of VEGFR-1 and VEGFR-2 in the aberrant hematopoiesis associated with elevated levels of VEGF. *Blood.* 110:624–631. https://doi.org/10.1182/blood-2007-01-065714

Kobayashi, H., Q. Liu, T.C. Binns, A.A. Urrutia, O. Davidoff, P.P. Kapitsinou, A.S. Pfaff, H. Olauson, A. Wernerson, A.B. Fogo, et al. 2016. Distinct subpopulations of FOXD1 stroma-derived cells regulate renal erythropoietin. *J. Clin. Invest.* 126:1926–1938. https://doi.org/10.1172/JCI83551

Koulnis, M., R. Pop, E. Porpiglia, J.R. Shearstone, D. Hidalgo, and M. Socolovsky. 2011. Identification and analysis of mouse erythroid progenitors using the CD71/TER119 flow-cytometric assay. *J. Vis. Exp.* (54):2809. https://doi.org/10.3791/2809

Koury, M.J., and M.C. Bondurant. 1990. Erythropoietin retards DNA breakdown and prevents programmed death in erythroid progenitor cells. *Science.* 248:378–381. https://doi.org/10.1126/science.2326648

Koury, M.J., and V.H. Haase. 2015. Anaemia in kidney disease: harnessing hypoxia responses for therapy. *Nat. Rev. Nephrol.* 11:394–410. https://doi.org/10.1038/nrneph.2015.82

Koury, S.T., M.C. Bondurant, and M.J. Koury. 1988. Localization of erythropoietin synthesizing cells in murine kidneys by in situ hybridization. *Blood.* 71:524–527.

Koury, S.T., M.C. Bondurant, M.J. Koury, and G.L. Semenza. 1991. Localization of cells producing erythropoietin in murine liver by in situ hybridization. *Blood.* 77:2497–2503 (see comments).

Kraft, A., K. Weindel, A. Ochs, C. Marth, J. Zmija, P. Schumacher, C. Unger, D. Marmé, and G. Gastl. 1999. Vascular endothelial growth factor in the sera and effusions of patients with malignant and nonmalignant disease. *Cancer.* 85:178–187. https://doi.org/10.1002/(SICI)1097-0142(19990101)85:1%3C178::AID-CNCR25%3E3.0.CO;2-7

Greenwald et al.
VEGF expands erythropoiesis via Epo induction

Journal of Experimental Medicine
https://doi.org/10.1084/jem.20180752

229

Kramann, R., and B.D. Humphreys. 2014. Kidney pericytes: roles in regeneration and fibrosis. *Semin. Nephrol.* 34:374–383. https://doi.org/10.1016/j.semnephrol.2014.06.004

Kramann, R., R.K. Schneider, D.P. DiRocco, F. Machado, S. Fleig, P.A. Bondzie, J.M. Henderson, B.L. Ebert, and B.D. Humphreys. 2015. Perivascular Gli1+ progenitors are key contributors to injury-induced organ fibrosis. *Cell Stem Cell.* 16:51–66. https://doi.org/10.1016/j.stem.2014.11.004

Kramann, R., C. Goettsch, J. Wongboonsin, H. Iwata, R.K. Schneider, C. Kuppe, N. Kaesler, M. Chang-Panesso, F.G. Machado, S. Gratwohl, et al. 2016. Adventitial MSC-like Cells Are Progenitors of Vascular Smooth Muscle Cells and Drive Vascular Calcification in Chronic Kidney Disease. *Cell Stem Cell.* 19:628–642. https://doi.org/10.1016/j.stem.2016.08.001

Kurt, B., K. Gerl, C. Karger, I. Schwarzensteiner, and A. Kurtz. 2015. Chronic hypoxia-inducible transcription factor-2 activation stably transforms juxtaglomerular renin cells into fibroblast-like cells in vivo. *J. Am. Soc. Nephrol.* 26:587–596. https://doi.org/10.1681/ASN.2013111152

Lacombe, C., J.L. Da Silva, P. Bruneval, J.G. Fournier, F. Wendling, N. Casadevall, J.P. Camilleri, J. Bariety, B. Varet, and P. Tambourin. 1988. Peritubular cells are the site of erythropoietin synthesis in the murine hypoxic kidney. *J. Clin. Invest.* 81:620–623. https://doi.org/10.1172/JCI113363

Leyland-Jones, B., V. Semiglazov, M. Pawlicki, T. Pienkowski, S. Tjulandin, G. Manikhas, A. Makhson, A. Roth, D. Dodwell, J. Baselga, et al. 2005. Maintaining normal hemoglobin levels with epoetin alfa in mainly nonanemic patients with metastatic breast cancer receiving first-line chemotherapy: a survival study. *J. Clin. Oncol.* 23:5960–5972. https://doi.org/10.1200/JCO.2005.06.150

Maktouf, C., A. Bounemra, S. Mahjoub, F. Msadek, A. Khlif, M. Karoui, S. Hdiji, S. Zriba, N.B. Romdhane, and M. Elloumi. 2011. Evaluation of serum VEGF levels in untreated erythrocytosis patients. *Pathol. Biol. (Paris).* 59:240–242. https://doi.org/10.1016/j.patbio.2010.02.005

Maxwell, P.H., C.W. Pugh, and P.J. Ratcliffe. 1993. Inducible operation of the erythropoietin 3′ enhancer in multiple cell lines: evidence for a widespread oxygen-sensing mechanism. *Proc. Natl. Acad. Sci. USA.* 90:2423–2427. https://doi.org/10.1073/pnas.90.6.2423

May, D., V. Djonov, G. Zamir, M. Bala, R. Safadi, M. Sklair-Levy, and E. Keshet. 2011. A transgenic model for conditional induction and rescue of portal hypertension reveals a role of VEGF-mediated regulation of sinusoidal fenestrations. *PLoS One.* 6:e21478. https://doi.org/10.1371/journal.pone.0021478

Nagai, T., Y. Yasuoka, Y. Izumi, K. Horikawa, M. Kimura, Y. Nakayama, T. Uematsu, T. Fukuyama, T. Yamazaki, Y. Kohda, et al. 2014. Reevaluation of erythropoietin production by the nephron. *Biochem. Biophys. Res. Commun.* 449:222–228. https://doi.org/10.1016/j.bbrc.2014.05.014

Nakamura, M., Y. Zhang, Y. Yang, C. Sonmez, W. Zheng, G. Huang, T. Seki, H. Iwamoto, B. Ding, L. Yin, et al. 2017. Off-tumor targets compromise antiangiogenic drug sensitivity by inducing kidney erythropoietin production. *Proc. Natl. Acad. Sci. USA.* 114:E9635–E9644. https://doi.org/10.1073/pnas.1703431114

Obara, N., N. Suzuki, K. Kim, T. Nagasawa, S. Imagawa, and M. Yamamoto. 2008. Repression via the GATA box is essential for tissue-specific erythropoietin gene expression. *Blood.* 111:5223–5232. https://doi.org/10.1182/blood-2007-10-115857

Paliege, A., C. Rosenberger, A. Bondke, L. Sciesielski, A. Shina, S.N. Heyman, L.A. Flippin, M. Arend, S.J. Klaus, and S. Bachmann. 2010. Hypoxia-inducible factor-2α-expressing interstitial fibroblasts are the only renal cells that express erythropoietin under hypoxia-inducible factor stabilization. *Kidney Int.* 77:312–318. https://doi.org/10.1038/ki.2009.460

Pan, X., N. Suzuki, I. Hirano, S. Yamazaki, N. Minegishi, and M. Yamamoto. 2011. Isolation and characterization of renal erythropoietin-producing cells from genetically produced anemia mice. *PLoS One.* 6:e25839. https://doi.org/10.1371/journal.pone.0025839

Panteli, K., M. Bai, E. Hatzimichael, N. Zagorianakou, N.J. Agnantis, and K. Bourantas. 2007. Serum levels, and bone marrow immunohistochemical expression of, vascular endothelial growth factor in patients with chronic myeloproliferative diseases. *Hematology.* 12:481–486. https://doi.org/10.1080/10245330701554664

Pennock, S., and A. Kazlauskas. 2012. Vascular endothelial growth factor A competitively inhibits platelet-derived growth factor (PDGF)-dependent activation of PDGF receptor and subsequent signaling events and cellular responses. *Mol. Cell. Biol.* 32:1955–1966. https://doi.org/10.1128/MCB.06668-11

Pinczewski, J., and J.C. Papadimitriou. 2011. Aberrant VEGF expression associated with neoplasm-induced extramedullary hematopoiesis in an epithelioid hemangioendothelioma: a case report. *Int. J. Surg. Pathol.* 19:662–666. https://doi.org/10.1177/1066896909356922

Prakash, S., N. Prasad, R.K. Sharma, R.M. Faridi, and S. Agrawal. 2012. Vascular endothelial growth factor gene polymorphisms in North Indian patients with end stage renal disease. *Cytokine.* 58:261–266. https://doi.org/10.1016/j.cyto.2012.01.020

Rankin, E.B., C. Wu, R. Khatri, T.L.S. Wilson, R. Andersen, E. Araldi, A.L. Rankin, J. Yuan, C.J. Kuo, E. Schipani, and A.J. Giaccia. 2012. The HIF signaling pathway in osteoblasts directly modulates erythropoiesis through the production of EPO. *Cell.* 149:63–74. https://doi.org/10.1016/j.cell.2012.01.051

Rehn, M., Z. Kertész, and J. Cammenga. 2014. Hypoxic induction of vascular endothelial growth factor regulates erythropoiesis but not hematopoietic stem cell function in the fetal liver. *Exp. Hematol.* 42:941–944.e1. https://doi.org/10.1016/j.exphem.2014.08.002

Salven, P., H. Mänpää, A. Orpana, K. Alitalo, and H. Joensuu. 1997. Serum vascular endothelial growth factor is often elevated in disseminated cancer. *Clin. Cancer Res.* 3:647–651.

Semenza, G.L., S.T. Koury, M.K. Nejfelt, J.D. Gearhart, and S.E. Antonarakis. 1991. Cell-type-specific and hypoxia-inducible expression of the human erythropoietin gene in transgenic mice. *Proc. Natl. Acad. Sci. USA.* 88:8725–8729. https://doi.org/10.1073/pnas.88.19.8725

Senger, D.R. 2010. Vascular endothelial growth factor: much more than an angiogenesis factor. *Mol. Biol. Cell.* 21:377–379. https://doi.org/10.1091/mbc.e09-07-0591

Shweiki, D., A. Itin, D. Soffer, and E. Keshet. 1992. Vascular endothelial growth factor induced by hypoxia may mediate hypoxia-initiated angiogenesis. *Nature.* 359:843–845. https://doi.org/10.1038/359843a0

Souma, T., S. Yamazaki, T. Moriguchi, N. Suzuki, I. Hirano, X. Pan, N. Minegishi, M. Abe, H. Kiyomoto, S. Ito, and M. Yamamoto. 2013. Plasticity of renal erythropoietin-producing cells governs fibrosis. *J. Am. Soc. Nephrol.* 24:1599–1616. https://doi.org/10.1681/ASN.2013010030

Souma, T., M. Nezu, D. Nakano, S. Yamazaki, I. Hirano, H. Sekine, T. Dan, K. Takeda, G.-H. Fong, A. Nishiyama, et al. 2016. Erythropoietin Synthesis in Renal Myofibroblasts Is Restored by Activation of Hypoxia Signaling. *J. Am. Soc. Nephrol.* 27:428–438. https://doi.org/10.1681/ASN.2014121184

Spivak, J.L. 2005. The anaemia of cancer: death by a thousand cuts. *Nat. Rev. Cancer.* 5:543–555. https://doi.org/10.1038/nrc1648

Tam, B.Y.Y., K. Wei, J.S. Rudge, J. Hoffman, J. Holash, S.K. Park, J. Yuan, C. Hefner, C. Chartier, J.-S. Lee, et al. 2006. VEGF modulates erythropoiesis through regulation of adult hepatic erythropoietin synthesis. *Nat. Med.* 12:793–800. https://doi.org/10.1038/nm1428

Vandekerckhove, J., G. Courtois, S. Coulon, J.-A. Ribeil, and O. Hermine. 2009. Regulation of erythropoiesis. *In* Handbook on Disorders of Iron Homeostasis, Erythrocytes and Erythropoiesis. C. Beaumont, editor. European School of Hematology. 45–87. Available at http://www.esh.org/esh-handbook-on-disorders-of-iron-metabolism-2009/.

von Lindern, M., U. Schmidt, and H. Beug. 2004. Control of erythropoiesis by erythropoietin and stem cell factor: a novel role for Bruton's tyrosine kinase. *Cell Cycle.* 3:876–879.

Weidemann, A., Y.M. Kerdiles, K.X. Knaup, C.A. Rafie, A.T. Boutin, C. Stockmann, N. Takeda, M. Scadeng, A.Y. Shih, V.H. Haase, et al. 2009. The glial cell response is an essential component of hypoxia-induced erythropoiesis in mice. *J. Clin. Invest.* 119:3373–3383. https://doi.org/10.1172/JCI39378

Xue, Y., F. Chen, D. Zhang, S. Lim, and Y. Cao. 2009. Tumor-derived VEGF modulates hematopoiesis. *J. Angiogenes. Res.* 1:9. https://doi.org/10.1186/2040-2384-1-9

Xue, Y., S. Lim, Y. Yang, Z. Wang, L.D.E. Jensen, E.-M. Hedlund, P. Andersson, M. Sasahara, O. Larsson, D. Galter, et al. 2011. PDGF-BB modulates hematopoiesis and tumor angiogenesis by inducing erythropoietin production in stromal cells. *Nat. Med.* 18:100–110. https://doi.org/10.1038/nm.2575

Zhao, H., J. Feng, K. Seidel, S. Shi, O. Klein, P. Sharpe, and Y. Chai. 2014. Secretion of shh by a neurovascular bundle niche supports mesenchymal stem cell homeostasis in the adult mouse incisor. *Cell Stem Cell.* 14:160–173. https://doi.org/10.1016/j.stem.2013.12.013